JAN 7 1953

NACA

RESEARCH MEMORANDUM

FOR REFERENCE

TRANSONIC WIND-TUNNEL INVESTIGATION OF THE EFFECTS OF

WING INCIDENCE ANGLE ON THE CHARACTERISTICS

OF TWO WING-BODY COMBINATIONS

By Francis G. Morgan, Jr.

Langley Aeronautical Laboratory
Langley Field, Va.

NATIONAL ADVISORY COMMITTEE
FOR AERONAUTICS

WASHINGTON

January 5, 1953

NATIONAL ADVISORY COMMITTEE FOR AERONAUTICS

RESEARCH MEMORANDUM

TRANSONIC WIND-TUNNEL INVESTIGATION OF THE EFFECTS OF

WING INCIDENCE ANGLE ON THE CHARACTERISTICS

OF TWO WING-BODY COMBINATIONS

By Francis G. Morgan, Jr.

SUMMARY

An investigation has been made in the Langley 8-foot transonic tunnel of the effects of wing incidence on the aerodynamic characteristics of two representative wing-body combinations at Mach numbers from 0.60 to 1.13 and fuselage angles of attack from $-8°$ to $4°$. A $45°$ sweptback wing was tested at an incidence angle of $4°$ with respect to the body, and an unswept wing was tested at $3°$ of incidence. Comparisons have been made with data previously obtained with the wings at $0°$ incidence. At subsonic Mach numbers, the maximum lift-drag ratio for the $45°$ sweptback wing is reduced by the introduction of both positive and negative incidence angles, while the ratio is raised for the unswept wing by use of positive incidence. No material effects of incidence angles were measured at transonic speeds.

INTRODUCTION

As part of an investigation of the effects of various component variations on the wing-body interference at transonic speeds, a sweptback wing and an unswept wing were tested at angles of incidence of $4°$ and $3°$, respectively, with reference to a typical fuselage. Measurements were made of lift, drag, and pitching moment at Mach numbers from 0.60 to 1.13 and angles of attack from $-8°$ to $4°$ in the Langley 8-foot transonic tunnel. Comparable results obtained with the wings at $0°$ incidence may be found in references 1 and 2. Comparisons with these previous data are presented to show the effects of incidence angle on the aerodynamic characteristics, especially maximum lift-drag ratio, for low lift coefficients. The major purpose of this investigation was to determine the effects of wing incidence angle on wing-body interference.

SYMBOLS

C_D drag coefficient, D/qS

C_L lift coefficient, L/qS

C_{L_α} lift-curve slope per degree

C_m pitching-moment coefficient about $0.25\bar{c}$ point, $\dfrac{M_{\bar{c}/4}}{qSc}$

$\dfrac{\partial C_m}{\partial C_L}$ static-longitudinal-stability parameter

i incidence angle, deg

$\bar{c}$ wing mean aerodynamic chord, in.

D drag, lb

L lift, lb

$(L/D)_{max}$ maximum lift-drag ratio

M average free-stream Mach number

$M_{\bar{c}/4}$ pitching moment about $0.25\bar{c}$ point, in.-lb

P_b base pressure coefficient, $\dfrac{P_b - P_o}{q}$

p_o free-stream static pressure, lb/sq ft

p_b static pressure at model base, lb/sq ft

q free-stream dynamic pressure, $\frac{1}{2}\rho V^2$, lb/sq ft

R Reynolds number based on $\bar{c}$

S wing area, sq ft

V free-stream velocity, ft/sec

α   angle of attack of fuselage center line, dég

ρ   free-stream density, slugs/cu ft

APPARATUS AND METHODS

Tunnel

These tests were conducted in the Langley 8-foot transonic tunnel, which is a dodecagonal, single-return wind tunnel designed, through the use of longitudinal slots along the test section, to obtain aerodynamic data for a range of Mach numbers through the speed of sound without the usual choking and blockage effects associated with a conventional closed-throat type of wind tunnel. It operates at atmospheric stagnation pressures. A more complete description of the Langley 8-foot transonic tunnel may be found in reference 3.

Configurations

The sweptback wing investigated is the same as that used in reference 1. It has 45° sweepback of the 0.25-chord line, an aspect ratio of 4, a taper ratio of 0.6, and NACA 65A006 airfoil sections parallel to the model plane of symmetry. The unswept wing is the same as that used in reference 2 and has zero sweep of the 0.25-chord line, an aspect ratio of 4.0, and a taper ratio of zero. The streamwise sections of the wing are symmetrical, and consist of circular arcs of different radii joined at the 0.40-chord station in order to have the maximum thickness of 0.04 chord located at this point. Other dimensions are shown on the sketch of the configurations tested (fig. 1). Both wings were constructed of 14S-T aluminum alloy.

The fuselage used is the same as the basic fuselage used in references 1 and 2. The general dimensions of this fuselage are shown in figure 1.

The 45° sweptback wing was tested at an incidence angle of 4°, while the unswept wing was tested at 3°. Both wings were tested as midwing configurations, as shown in figure 2.

Measurements and Accuracy

The average free-stream Mach number was determined to within ±0.003.

Lift, drag, and pitching moment were determined by means of an electrical strain-gage balance located inside the body and attached to the

sting at the model base (fig. 2). The accuracy of the data obtained,
based on the static calibration of the balance and the reproducibility
of the data, is estimated to be within the following limits:

	Low Speed	High Speed
C_L	±0.008	±0.004
C_D	±0.001	±0.0005
C_m	±0.005	±0.003

These are maximum limits and the accuracy is usually much better.

The base pressure was determined from two static orifices located
on the top and bottom of the sting support in the plane of the model
base (fig. 1). The base pressure coefficient (fig. 3) was estimated to
be accurate within ±0.003.

The angle of attack of the model was measured by an optical cathe-
tometer sighted on a reference line on the side of the fuselage. The
cathetometer measured the angle of attack to within ±0.1°.

Test Conditions

The tests were conducted through a Mach number range from 0.60 to
approximately 1.13. The test Reynolds number, based on the mean aero-
dynamic chord of the wing, varied from approximately 1.61×10^6 to
1.94×10^6 for the 45° sweptback wing, and from approximately 1.67×10^6
to 2.01×10^6 for the unswept wing. The 45° sweptback wing was tested
at angles of attack from -8° to 4°, whereas the unswept wing was tested
from -7° to 4°. Both wings were tested at large enough negative angles
to allow the determination of the effect of negative incidence angles on
maximum lift-drag ratios.

RESULTS

Presentation of Results

The basic lift, drag, and pitching-moment data for the incidence
conditions are presented in figures 4 and 5. In order to facilitate
presentation of the data, staggered scales have been used in figures 3
to 5 and, therefore, care should be taken in identifying the zero axis
for each curve. Analysis of the effects of incidence angle is shown in
figures 6 to 11. Reference to wings in this discussion refers to data

presented for wing-body configurations. Data for the body-alone configuration can be found in reference 1.

Boundary Interference

The axially slotted test section of the Langley 8-foot transonic tunnel minimizes boundary interference due to solid blockage (ref. 4). The effects of wake blockage are similarly reduced. The corrections to the Mach number and the dynamic pressure for these effects and to the drag coefficient for the effect of pressure gradient caused by the wake are no longer necessary at low angles of attack.

Boundary interference effects at Mach numbers above 1.0 consisted of shocks and expansions from the model which are reflected back to the surface of the model by the test-section boundary. For the configurations tested, these disturbances passed aft of the model base at a Mach number of 1.1, and all data above this Mach number were interference free. However, even in the Mach number range where boundary-reflected disturbances reached the model, the effects on the comparisons of this data with the data for 0° angle of incidence were small. These discrepancies have been minimized by fairing the data, and it is believed that none of the general trends exhibited by these data or the conclusions drawn from them were affected by the boundary-reflected disturbances.

Base Pressure Adjustments

The drag data have been adjusted for base pressure so that the drag corresponds to conditions where the body base pressure is equal to the free-stream static pressure. The base pressure coefficients used to adjust these drag data are shown in figure 3.

DISCUSSION

Lift

Ratios of the change in lift coefficient due to wing incidence angle to the change caused by angle of attack are presented as figure 6. Less lift is obtained through the use of an incidence angle than is obtained for a corresponding angle of attack. This result is primarily caused by the absence of upflow at the wing leading edge for the incidence condition, since, as is shown in reference 1, the lift of the fuselage is negligible. Generally, there is little variation of lift-curve slope associated with the changes in incidence angle (fig. 7). For the unswept wing at a lift coefficient of 0.4, the values are lower for the incidence

condition in the subsonic Mach number range and higher in the transonic range.

Pitching Moment

The variation of the pitching-moment coefficient at a constant lift coefficient (fig. 8) indicates that incidence reduces the pitching-moment coefficient a constant amount over the entire Mach number range. This result is attributable to changes in fuselage loads. The variation of the static-longitudinal-stability parameter with Mach number at zero lift is more gradual for the incidence condition (fig. 9), and it indicates a more stable configuration for this condition. At a higher lift coefficient, the values are approximately the same.

Drag

The drag coefficient for a constant lift coefficient, presented in figure 10, is affected very little by the change in incidence angle for either wing tested.

The wing incidence angles investigated have small, but significant, effects on the maximum lift-drag ratio (fig. 11). For the 45° sweptback wing, both positive and negative incidence angles reduce this ratio in the subsonic speed range. At transonic speeds, incidence has only a negligible effect. For the unswept wing at subsonic speeds, positive incidence angles give an increase in maximum lift-drag ratio, while negative incidence angles produce a decrease. However, in the transonic speed range, neither positive nor negative wing incidence angles have any material effect.

Limitations of Results

Results presented are for low angles of attack only. At higher angles of attack, the effects of incidence may be greater than those presented herein.

CONCLUSIONS

A transonic wind-tunnel investigation of the effects of wing incidence angle on the characteristics of two wing-body combinations, one

with a 45° sweptback wing and one with an unswept wing, at low angles of attack, leads to the following conclusions:

1. An increase in incidence angle produces less lift than a corresponding increase in angle of attack.

2. Wing incidence angle lowers the pitching-moment coefficient, for a constant lift coefficient, a constant amount throughout the entire Mach number range.

3. In the transonic speed range, neither positive nor negative incidence angles have any material effects on the lift-drag ratio for either wing. For the 45° sweptback wing, both positive and negative incidence angles decrease the maximum lift-drag ratio in the subsonic speed range. For the unswept wing, in the subsonic speed range, positive incidence angles increase this ratio, while negative incidence angles decrease it. This difference in the effects for the two wings is not necessarily an effect of sweep, because other parameters varied also.

Langley Aeronautical Laboratory,
        National Advisory Committee for Aeronautics,
            Langley Field, Va.

REFERENCES

1. Loving, Donald L., and Wornom, Dewey E.: Transonic Wind-Tunnel Investigation of the Interference Between a 45° Sweptback Wing and a Systematic Series of Four Bodies. NACA RM L52J01, 1952.

2. Estabrooks, Bruce B.: Transonic Wind-Tunnel Investigation of an Unswept Wing in Combination With a Systematic Series of Four Bodies. NACA RM L52K12a, 1952.

3. Wright, Ray H., and Ritchie, Virgil S.: Characteristics of a Transonic Test Section With Various Slot Shapes in the Langley 8-Foot High-Speed Tunnel. NACA RM L51H10, 1951.

4. Wright, Ray H., and Ward, Vernon G.: NACA Transonic Wind-Tunnel Test Sections. NACA RM L8J06, 1948.

|← 17.00 →|← 12.00 →|

12.00

32.605

(b) Unswept wing.
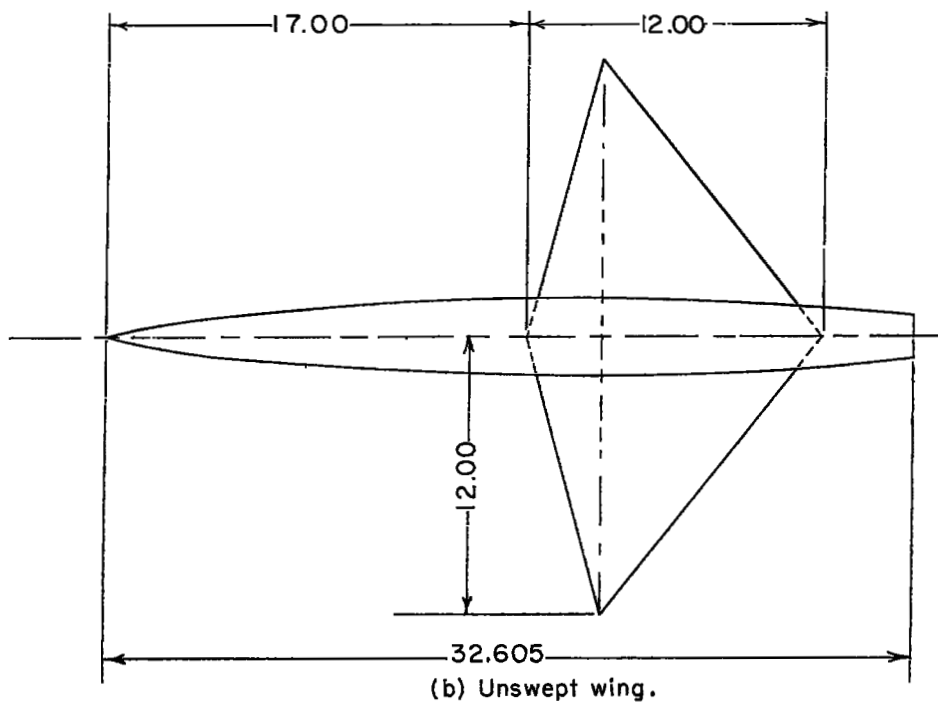
Configuration Details

|	Wing (a)	Wing (b)
Area, sq ft	1	1
Aspect ratio	4	4
Mean aerodynamic chord, in.	6.125	6.000
Taper ratio	.6	0
Area of model base, sq ft	0.0192	0.0192

7.50

Base pressure orifice

$Diam._{max} = 3.33$

45°

12.00

12.63

4.50

(a) 45° sweptback wing.

NACA
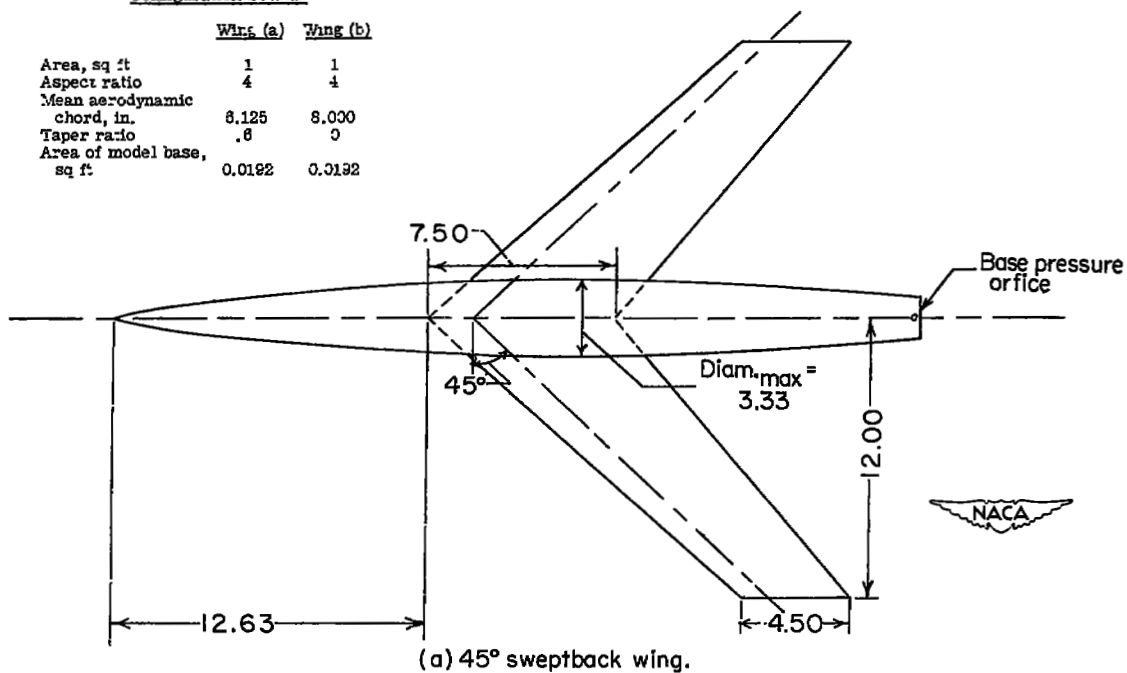
Figure 1.- Wing-body configurations used in investigation. All linear dimensions are in inches.

NACA
L-72970

Figure 2.- The wing-body combination with 45° sweptback wing, mounted in the test section of the 8-foot transonic tunnel.
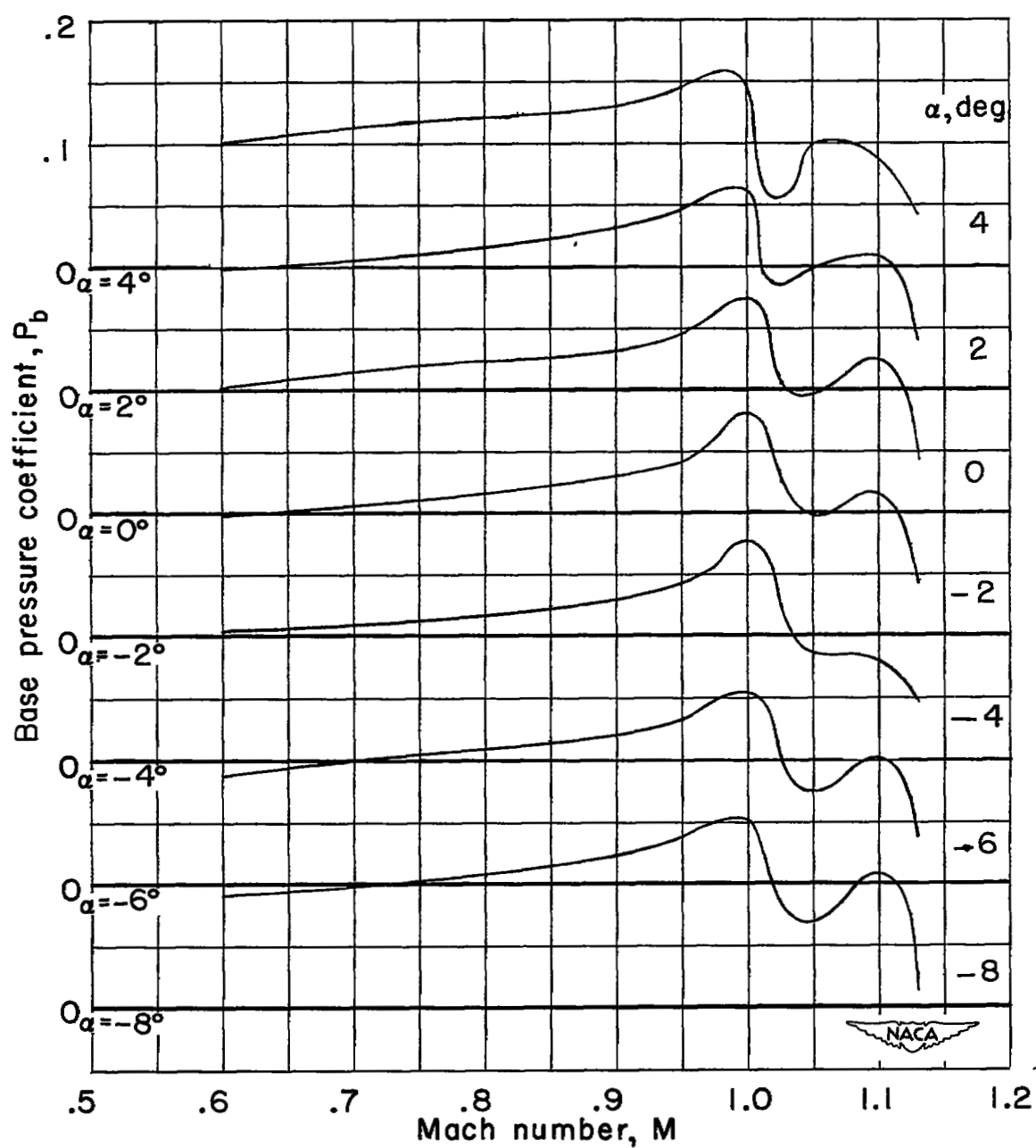
(a) 45° sweptback wing.

Figure 3.- Variation with Mach number of the base pressure coefficient
for the wing-body combinations.
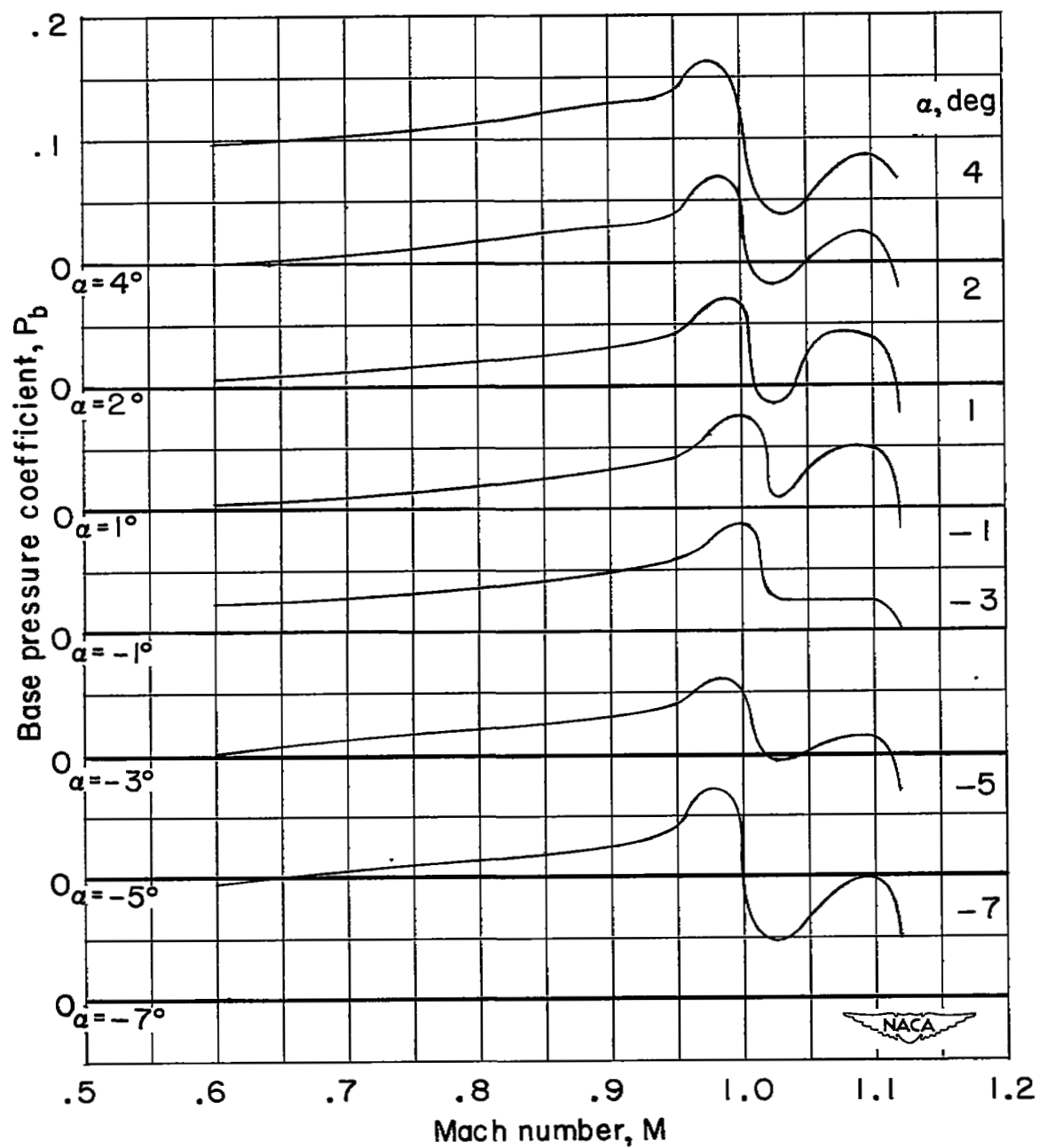
(b) Unswept wing.

Figure 3.- Concluded.
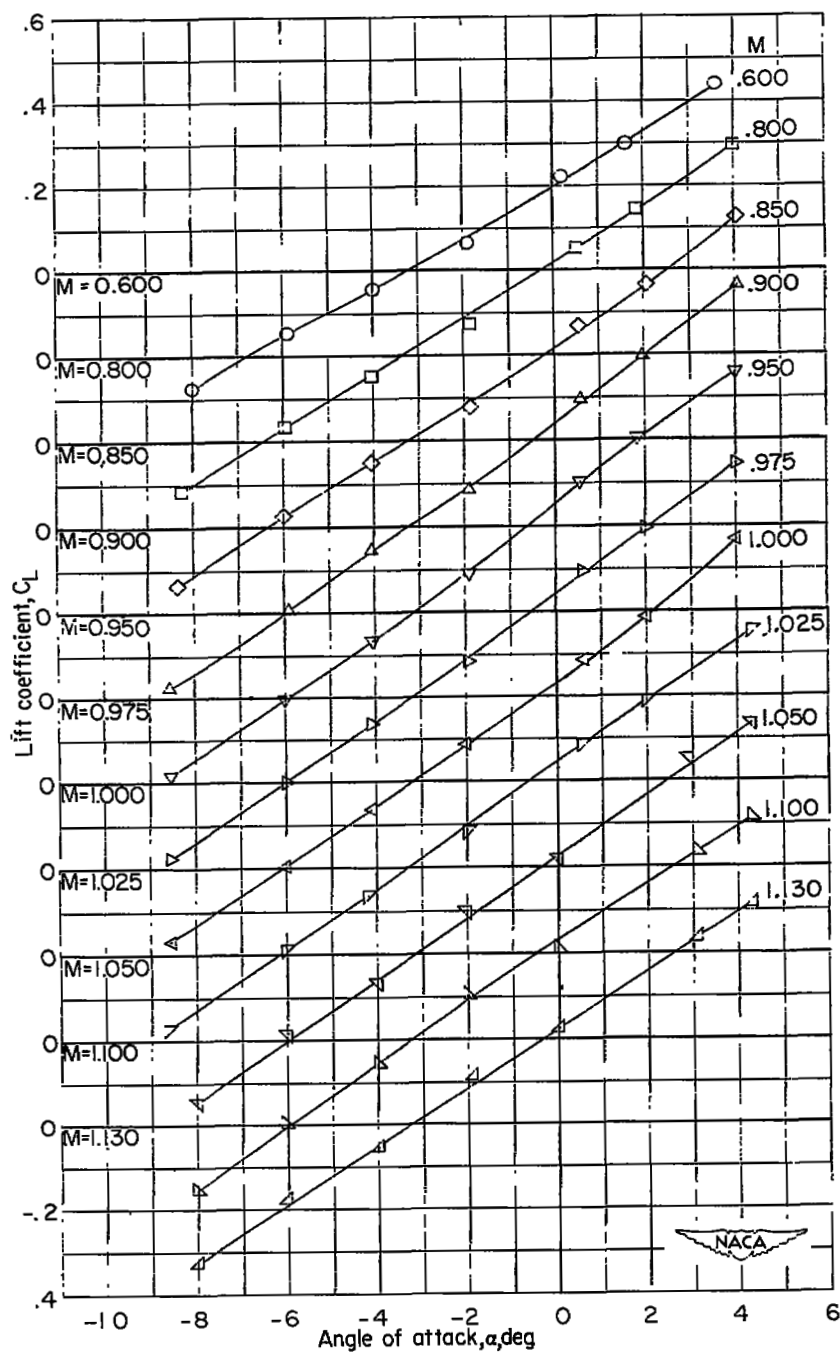
(a) Lift coefficient.

Figure 4.- Aerodynamic characteristics of the wing-body combination with
45° sweptback wing.   i = 4°.
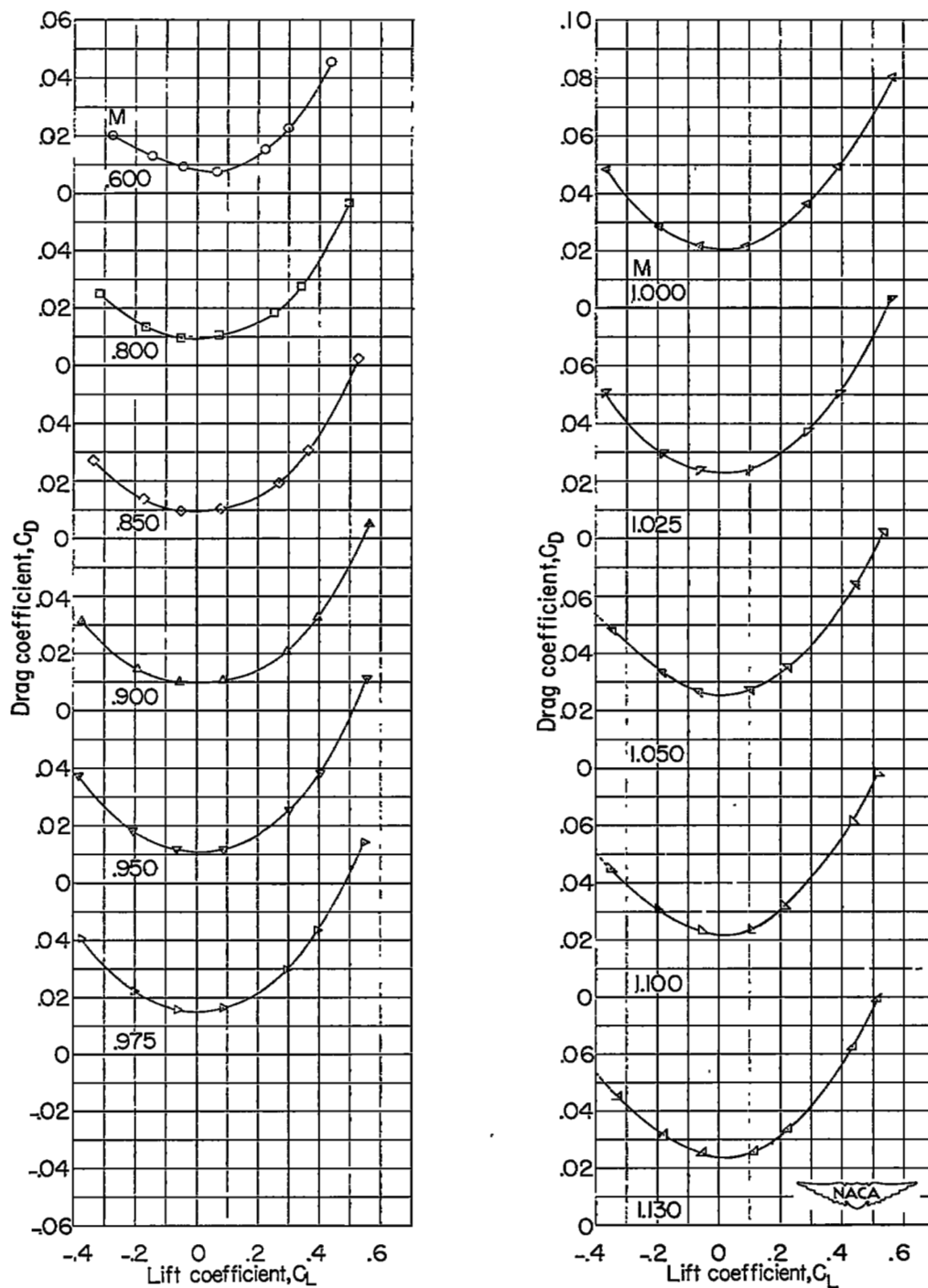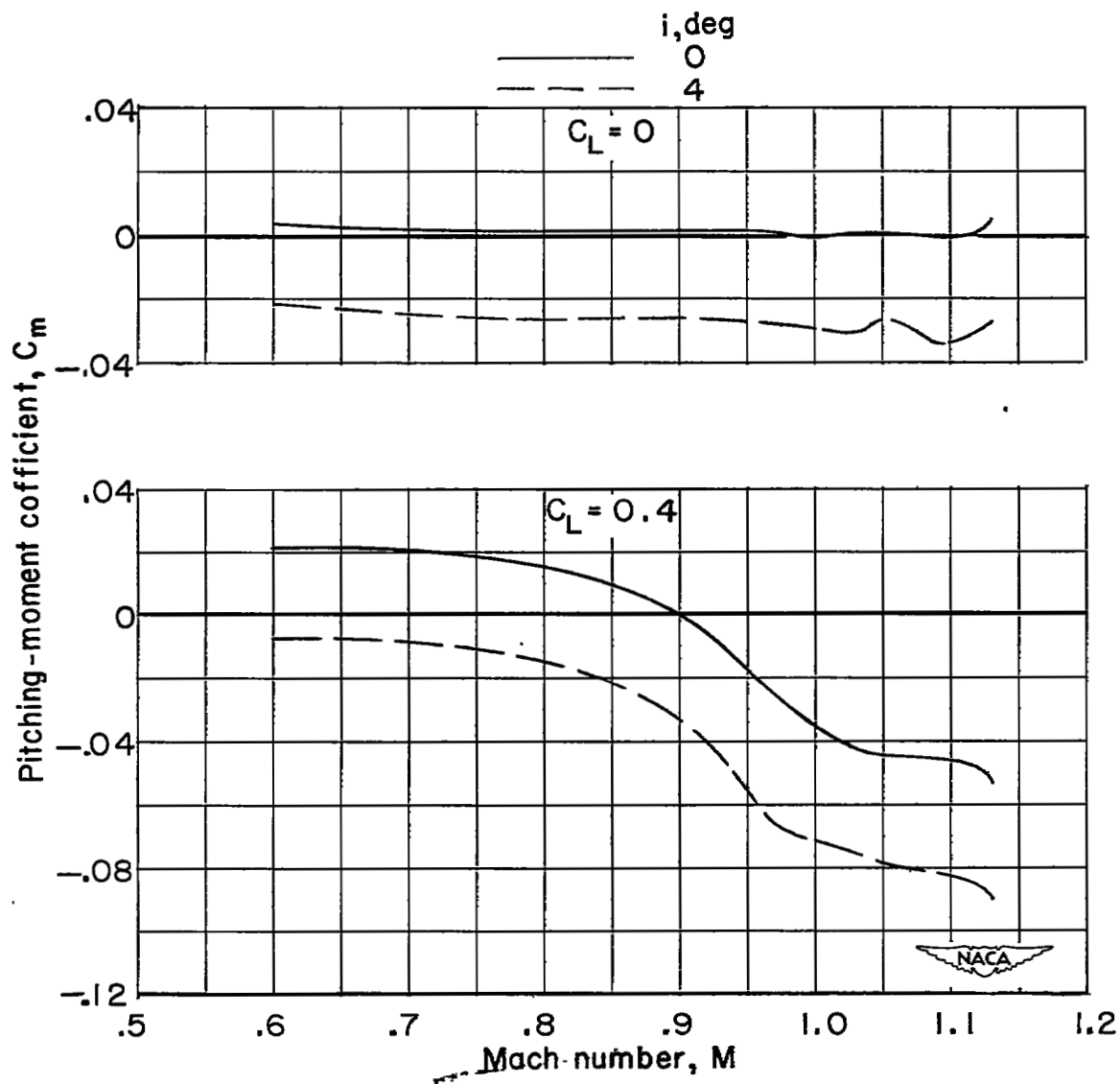
(b) Drag coefficient.

Figure 4.- Continued.
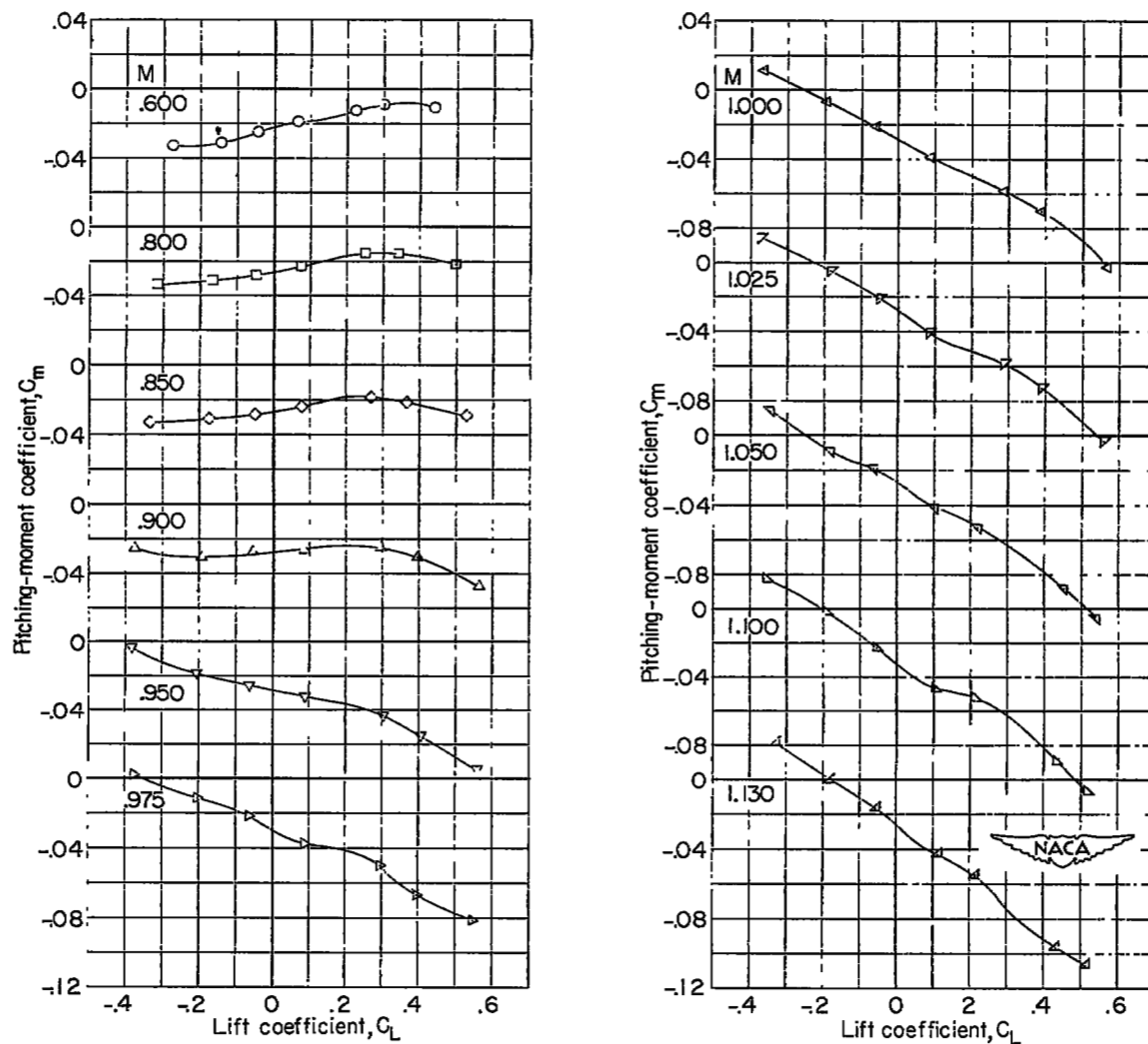
(c) Pitching-moment coefficient.

Figure 4.- Concluded.
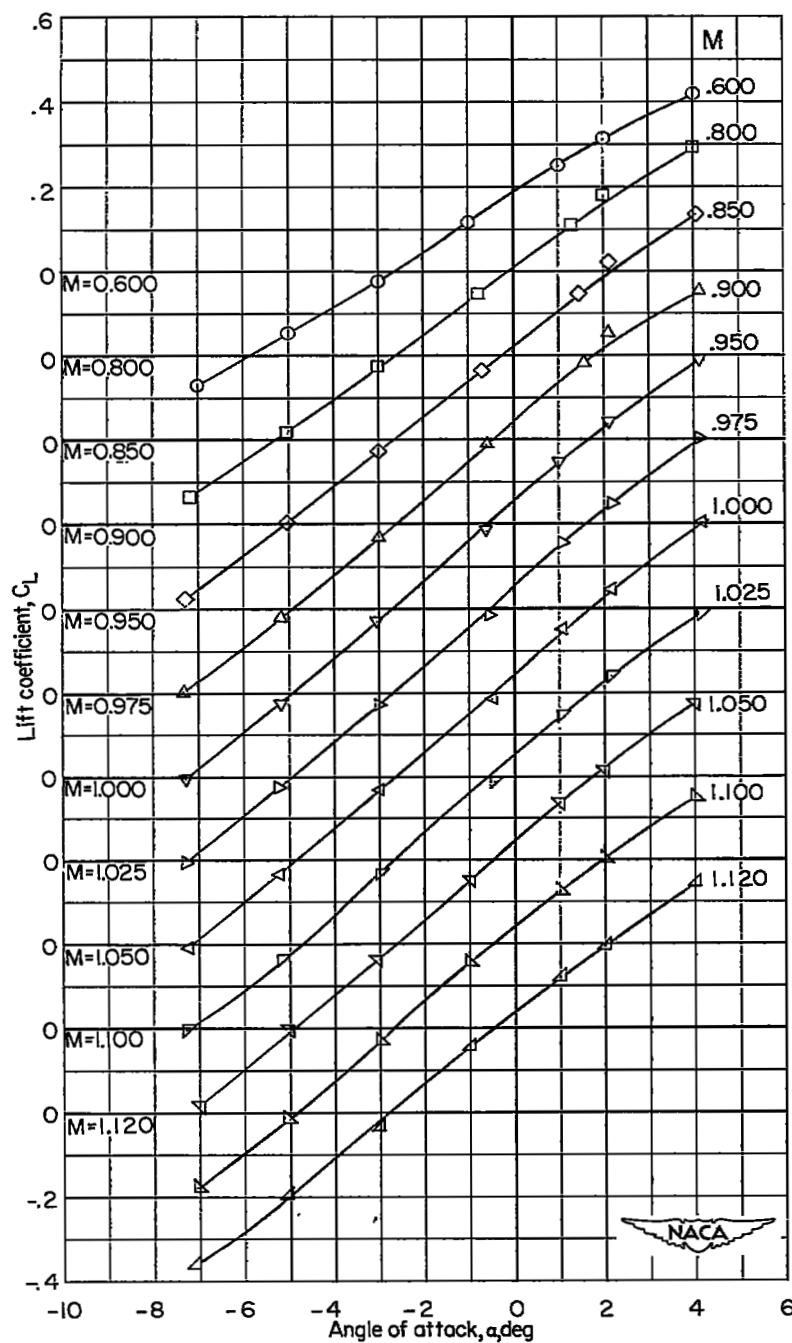
(a) Lift coefficient.

Figure 5.- Aerodynamic characteristics of the wing-body combination with unswept wing. i = 3°.
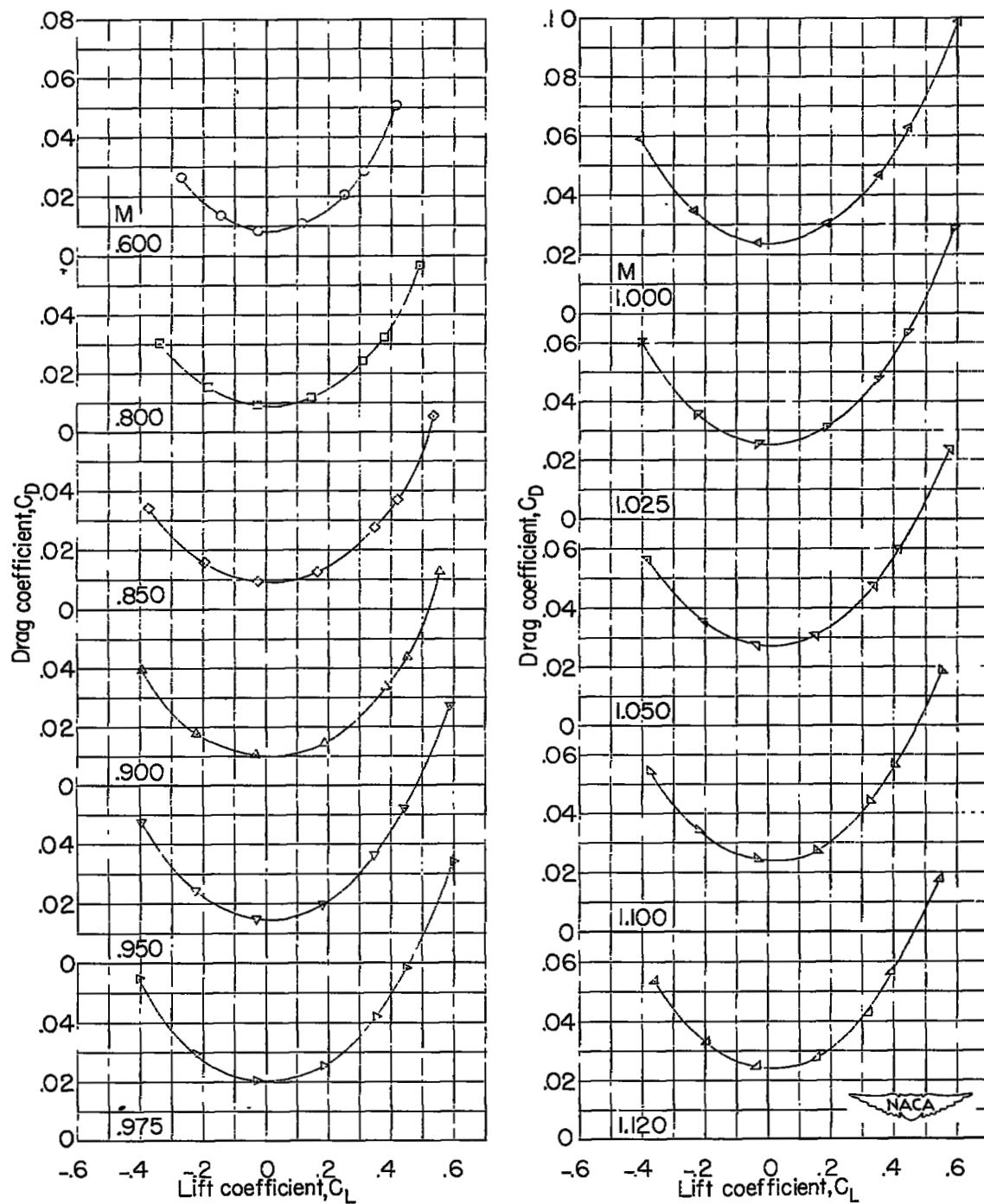
(b) Drag coefficient.

Figure 5.- Continued.
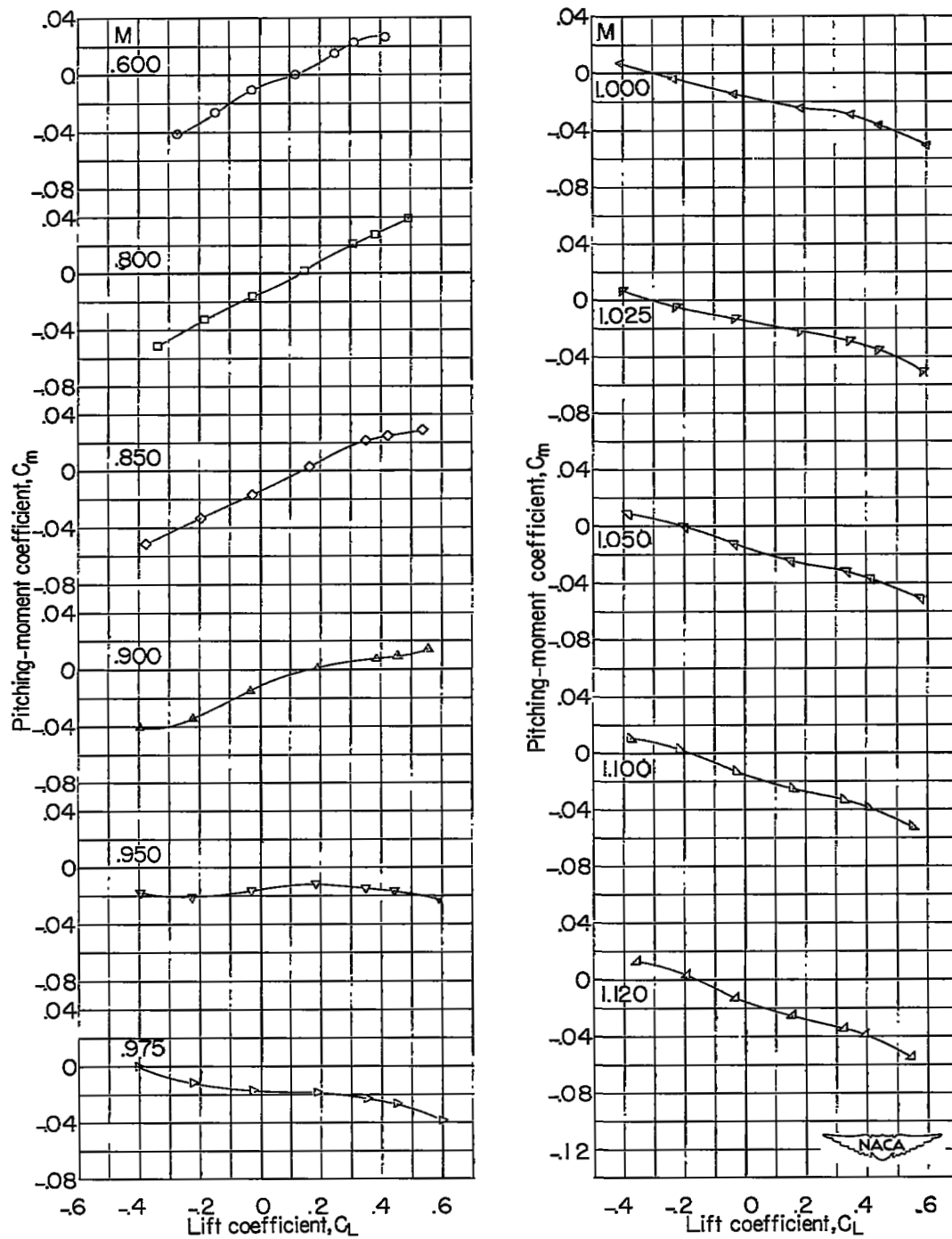
(c) Pitching-moment coefficient.

Figure 5.- Concluded.
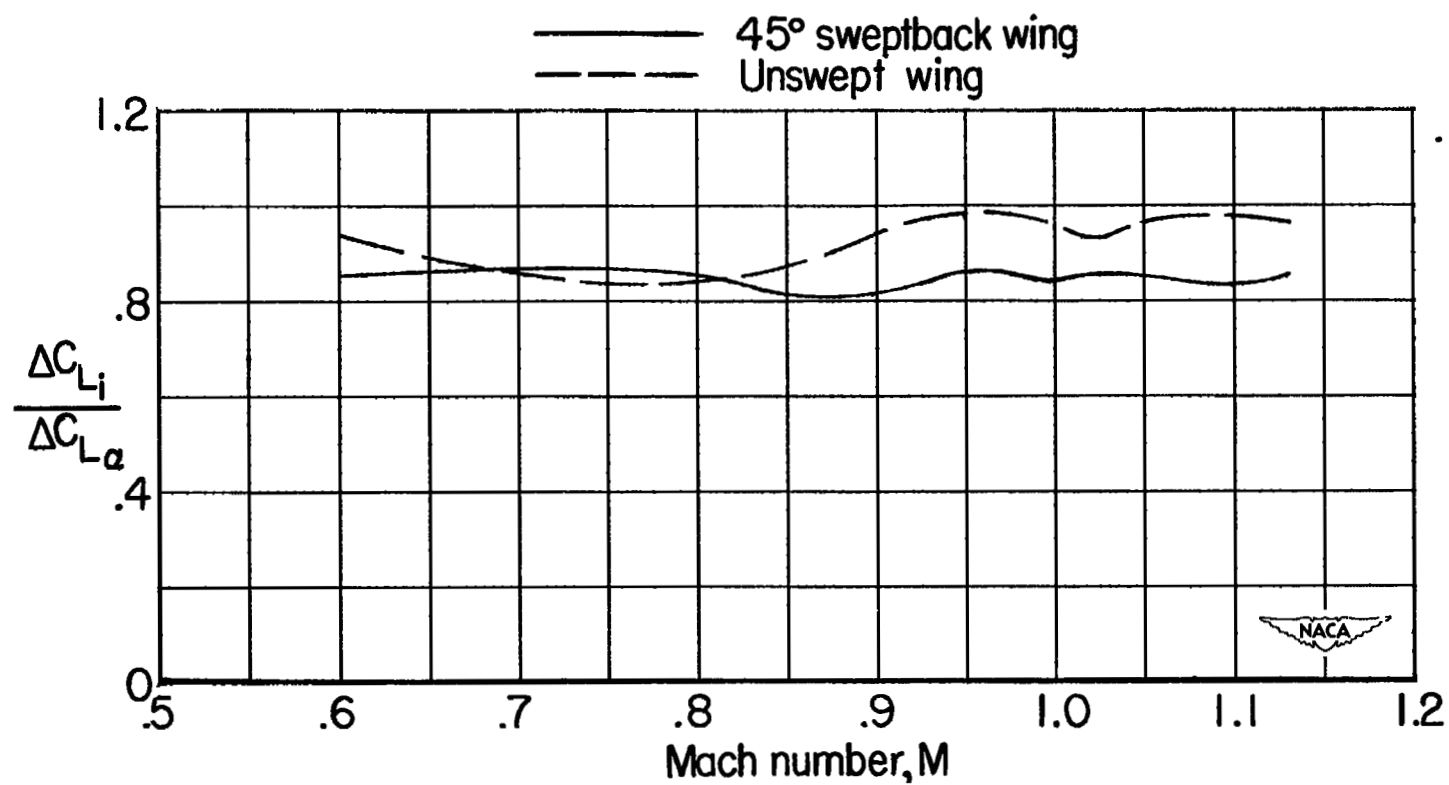
Figure 6.- Ratio of lift associated with angle of incidence to lift
associated with angle of attack.
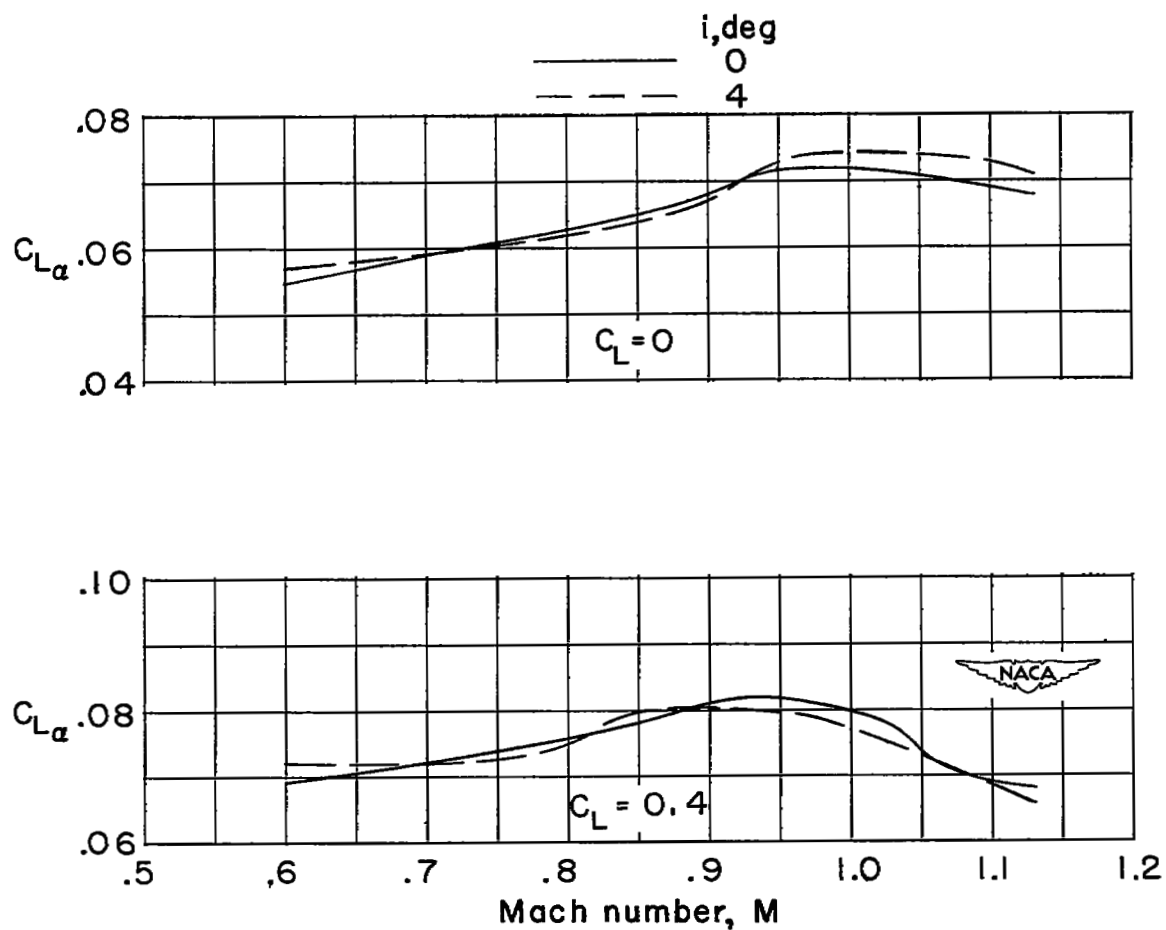
(a) 45° sweptback wing.

Figure 7.- Variation with Mach number of the lift-curve slope for the
wing-body combinations.
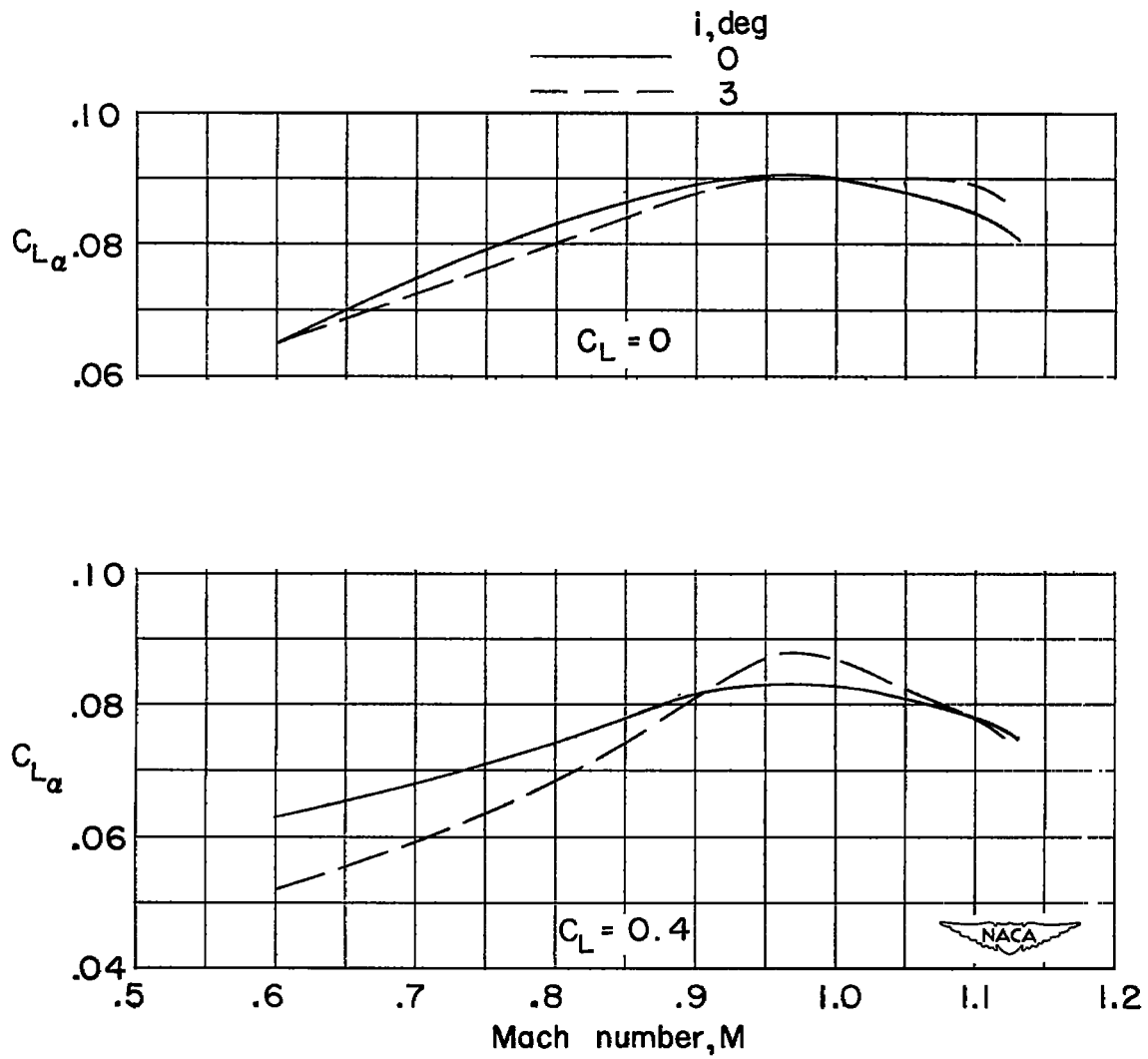
(b) Unswept wing.

Figure 7.- Concluded.

(a) 45° sweptback wing.

Figure 8.- Variation with Mach number of the pitching-moment coefficient for the wing-body combinations.
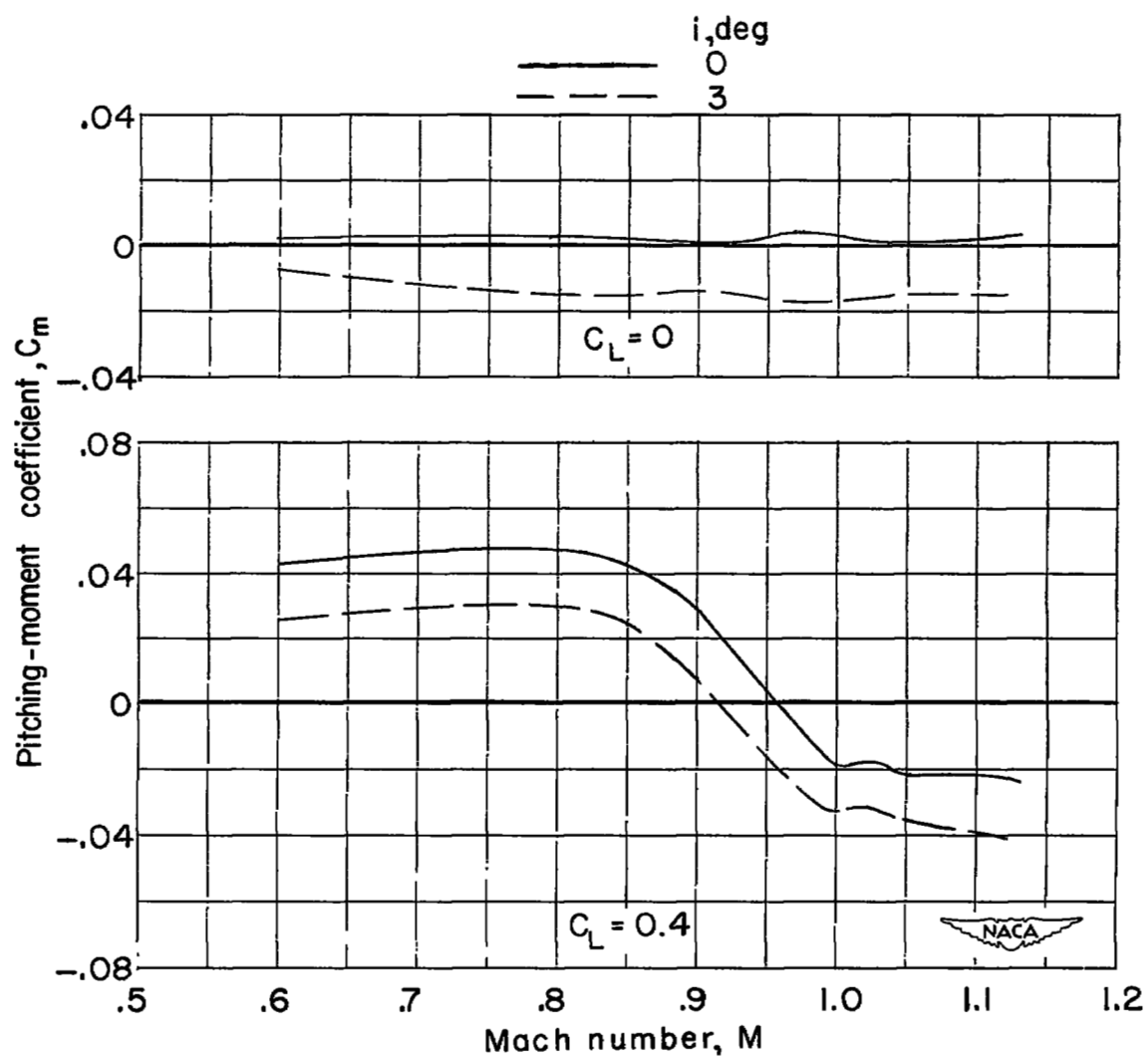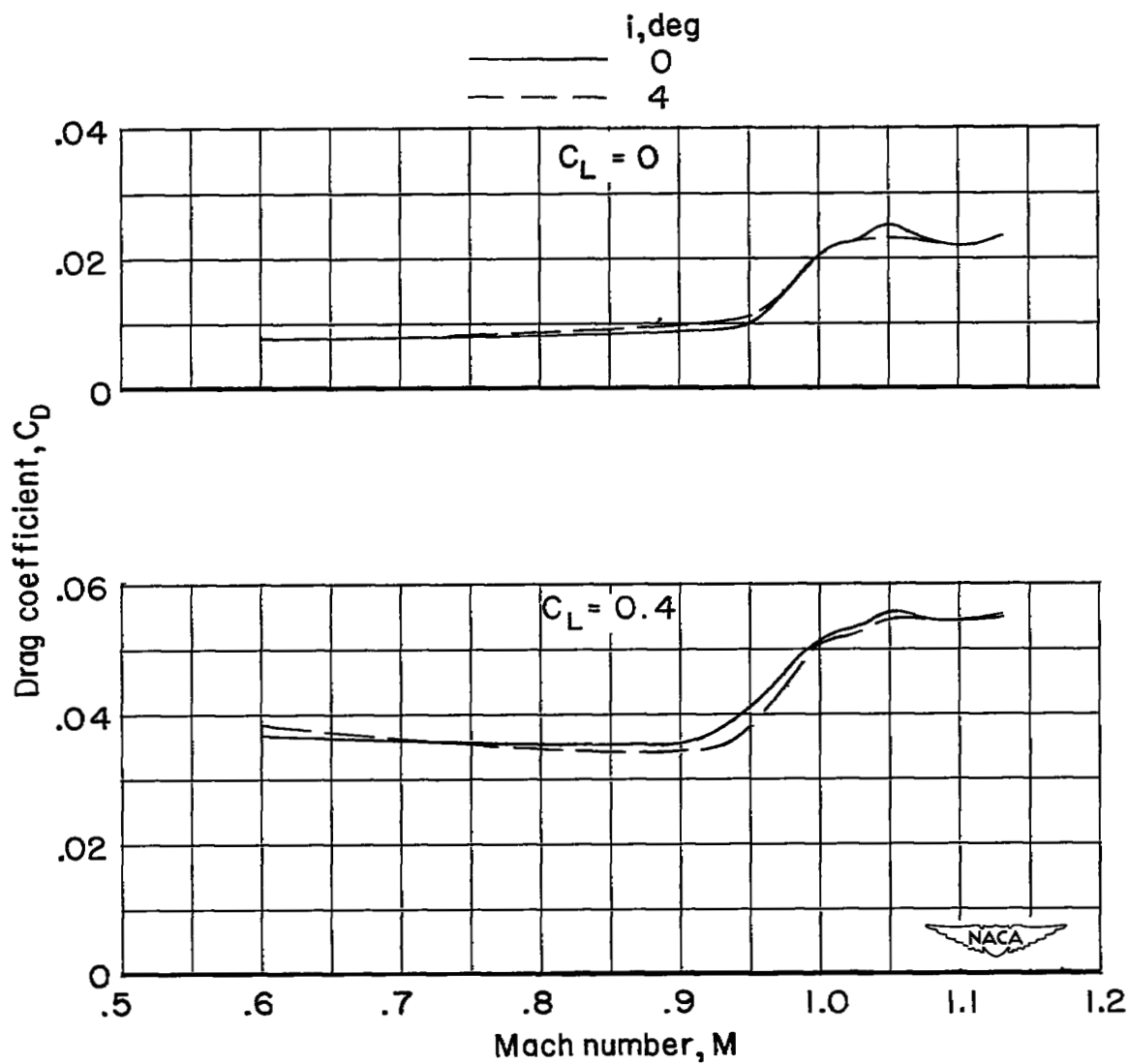
(b) Unswept wing.

Figure 8.- Concluded.
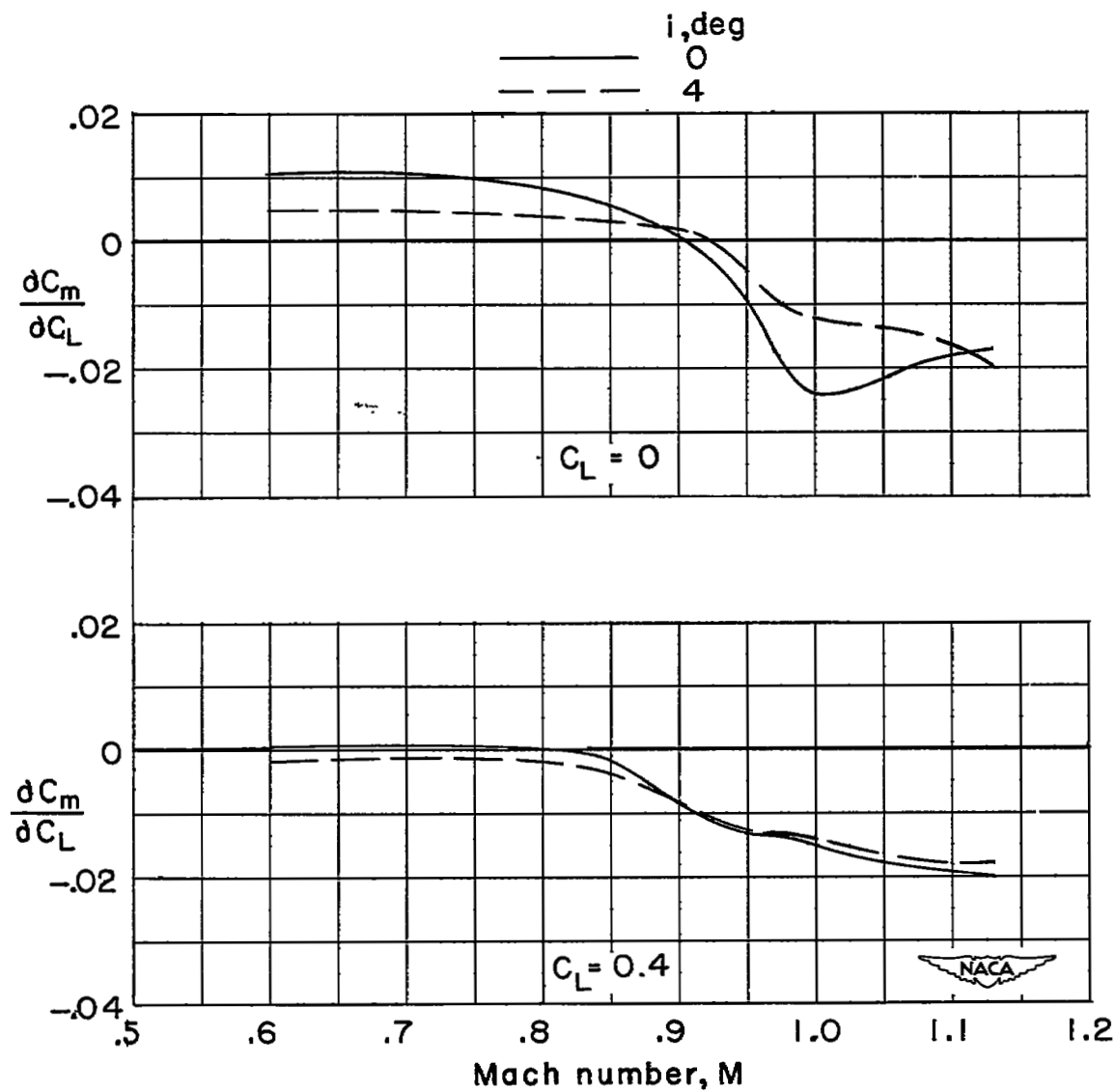
(a) 45° sweptback wing.

Figure 9.- Variation with Mach number of the static-longitudinal-stability
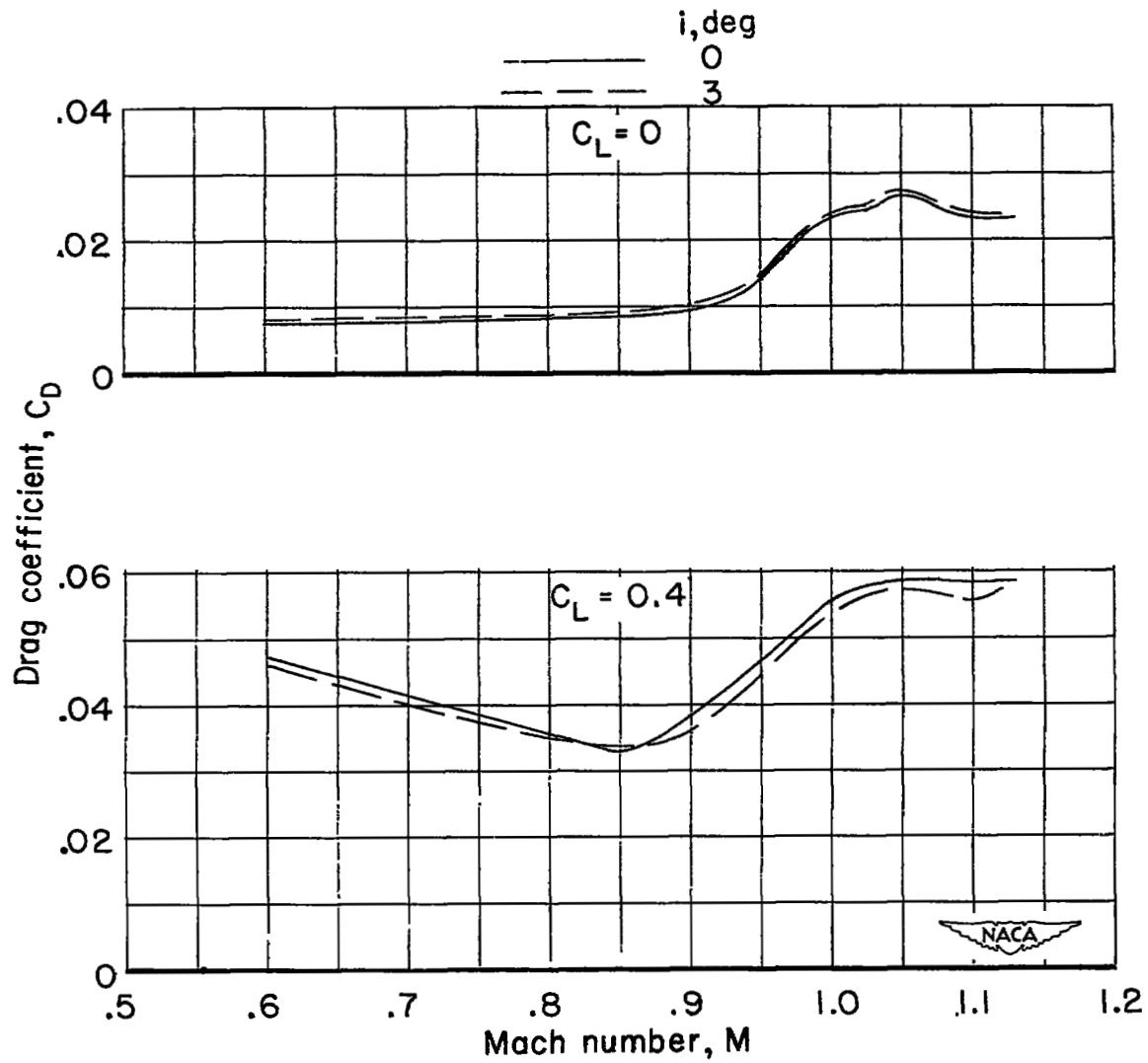parameter for the wing-body combinations.
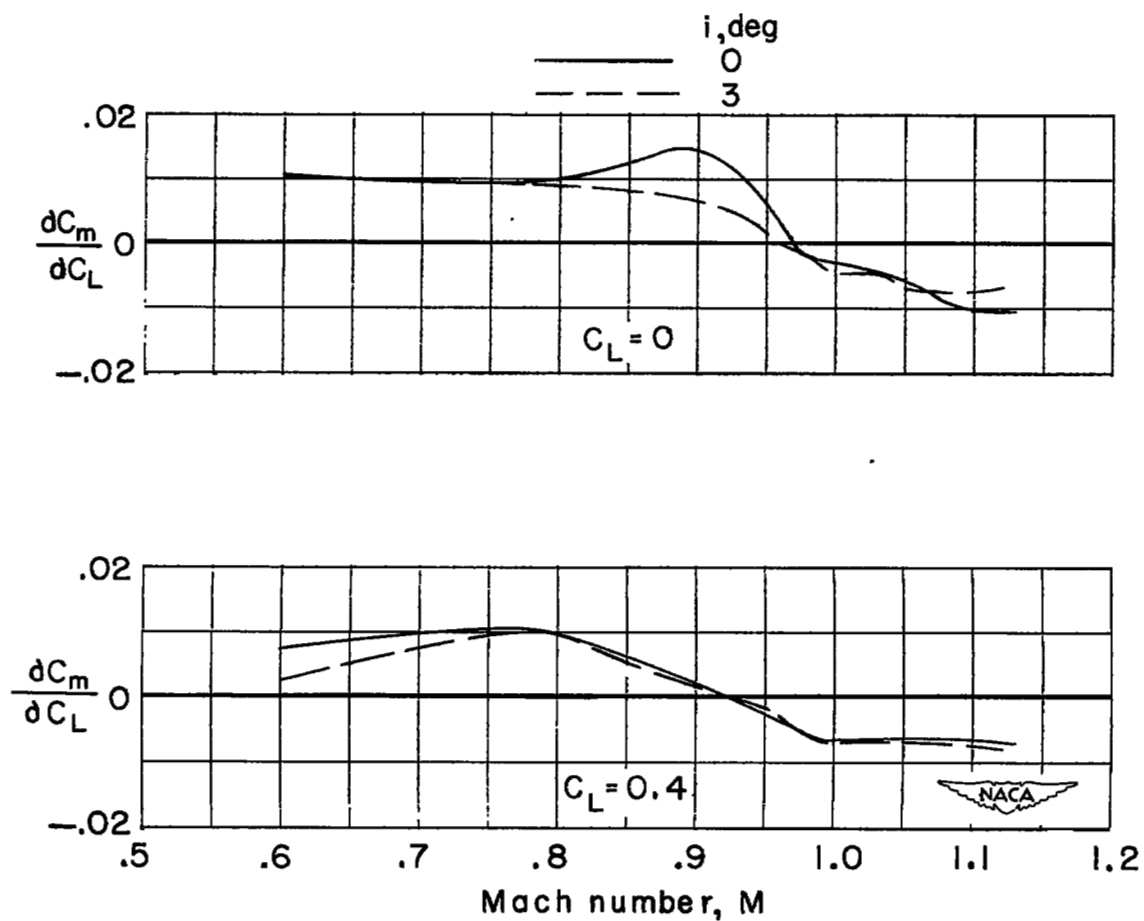
(b) Unswept wing.

Figure 9.- Concluded.

i,deg
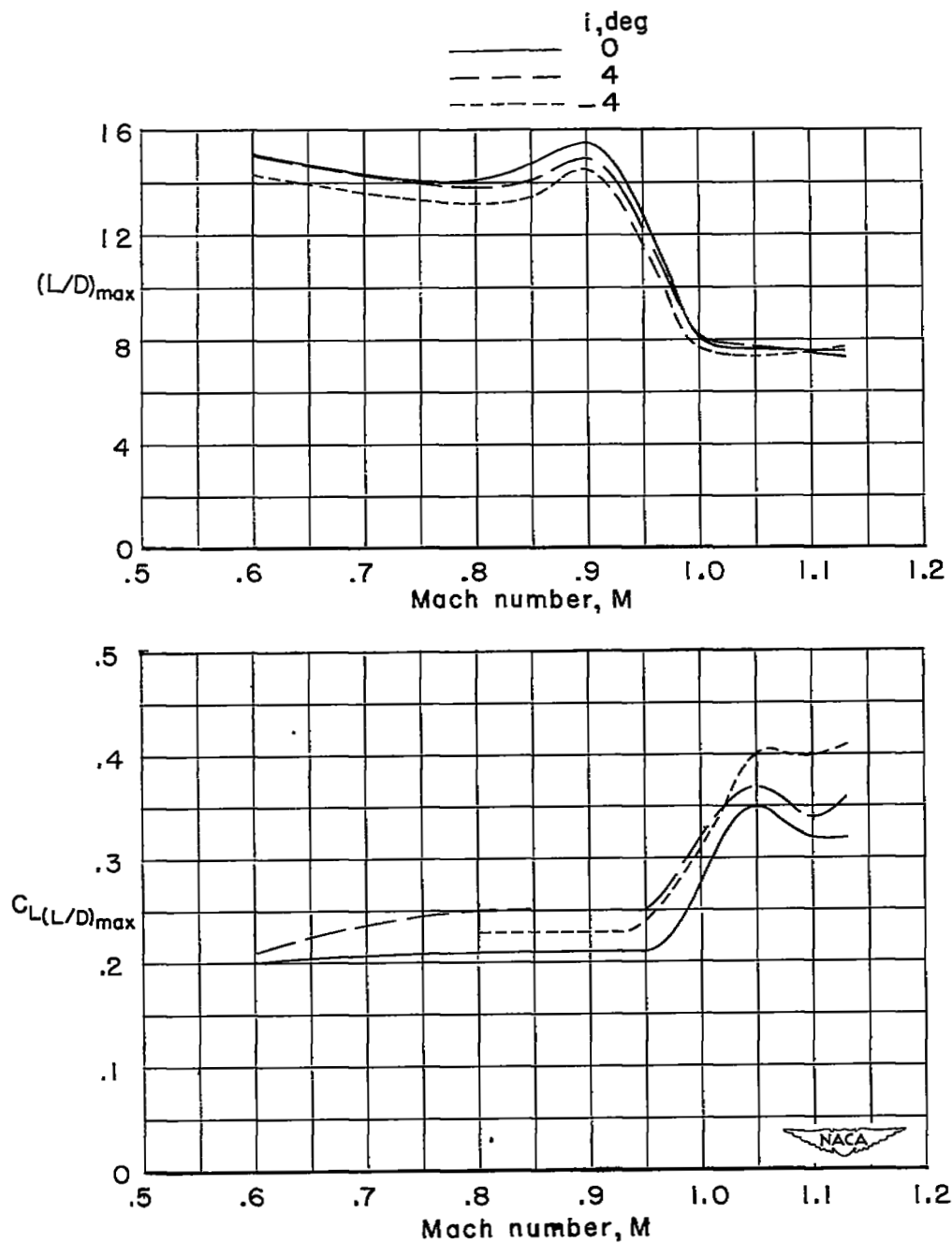——————   O
— — —   4

(a) 45° sweptback wing.

Figure 10.- Variation with Mach number of the drag coefficient for a
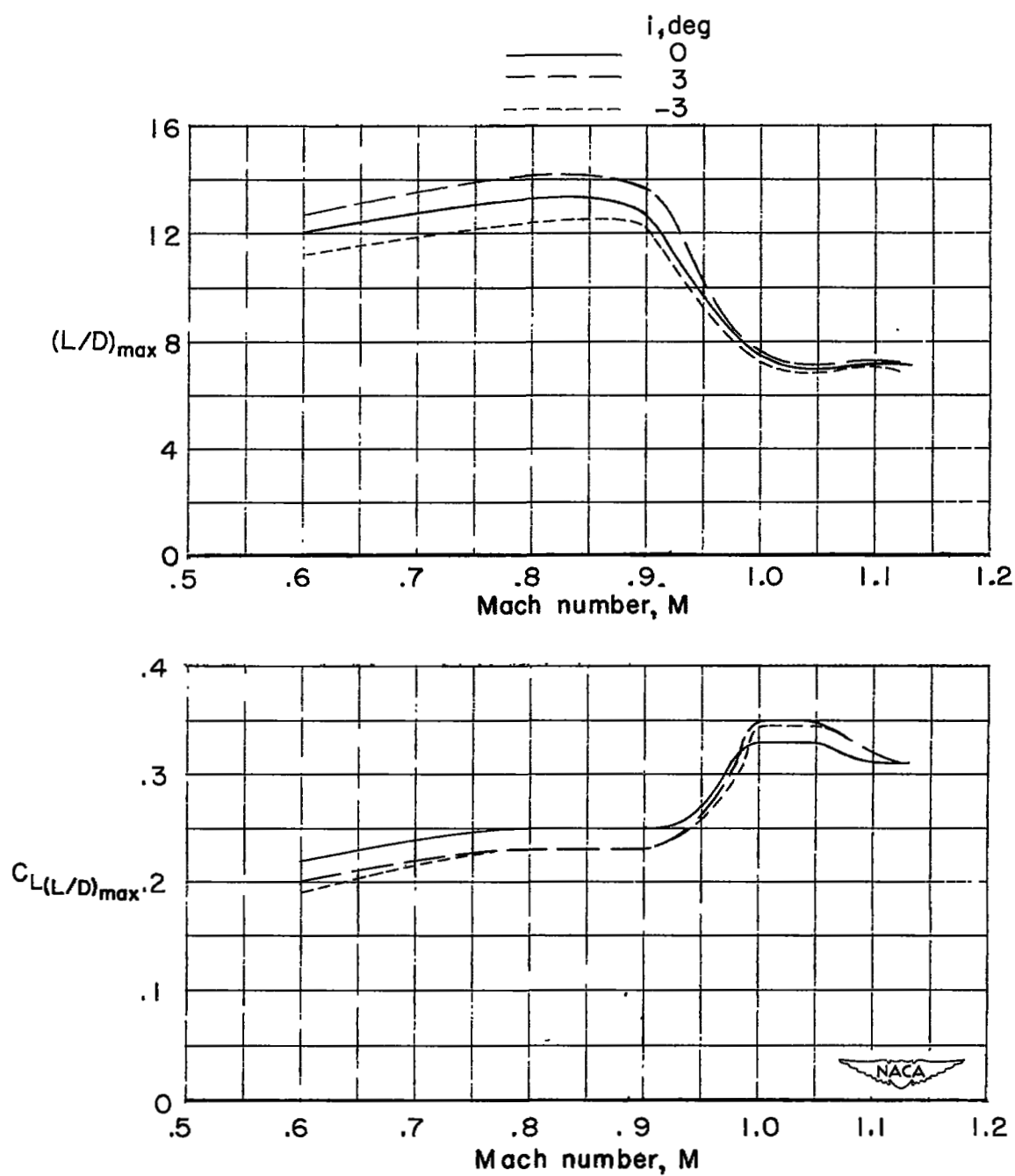given lift coefficient for the wing-body combinations.

(b) Unswept wing.

Figure 10.- Concluded.

(a) 45° sweptback wing.

Figure 11.- Variation with Mach number of maximum lift-drag ratio and
   of lift coefficient for maximum lift-drag ratio for the wing-body
   configurations.

(b) Unswept wing.

Figure 11.- Concluded.